Generation of controlled delaminations in composites using symmetrical laser shock configuration

Meriem Ghrib, Laurent Berthe, Nazih Mechbal, Marc Rebillat, M Guskov, Romain Ecault, Nas Bedreddine

▶ **To cite this version:**

Meriem Ghrib, Laurent Berthe, Nazih Mechbal, Marc Rebillat, M Guskov, et al.. Generation of controlled delaminations in composites using symmetrical laser shock configuration. Composite Structures, 2017, 171, pp.286-297. 10.1016/j.compstruct.2017.03.039 . hal-01662852

HAL Id: hal-01662852
https://hal.science/hal-01662852

Submitted on 13 Dec 2017

HAL is a multi-disciplinary open access archive for the deposit and dissemination of scientific research documents, whether they are published or not. The documents may come from teaching and research institutions in France or abroad, or from public or private research centers.

L'archive ouverte pluridisciplinaire **HAL**, est destinée au dépôt et à la diffusion de documents scientifiques de niveau recherche, publiés ou non, émanant des établissements d'enseignement et de recherche français ou étrangers, des laboratoires publics ou privés.

Generation of controlled delaminations in composites using symmetricallaser shock configuration

Meriem Ghrib [a,*], Laurent Berthe [a], Nazih Mechbal [a], Marc Rébillat [a], Mikhail Guskov [a], Romain Ecault [b], Nas Bedreddine [c]

[a] Processes and Engineering in Mechanics and Materials laboratory, UMR CNRS 8006, 151 Bd de l'hôpital, 75013 Paris, France
[b] Airbus Group Innovation, 18 rue Marius Tercé, 31025 Toulouse, France
[c] SAFRAN Nacelles, Département Matériaux et Procédés, Route du Pont VIII, 76700 Gonfreville-l'Orcher, France

Article history:
Received 10 September 2016
Revised 8 February 2017
Accepted 8 March 2017
Available online 16 March 2017

Keywords:
SHM
CFRP composite laminates
Delamination
Quantification algorithms
Damage calibration
Symmetrical laser shock
Post mortem analyses

A B S T R A C T

Structural Health Monitoring (SHM) is defined as the process of implementing a damage identification strategy for aerospace, civil and mechanical engineering infrastructures. SHM can be organized into five main steps: detection, localization, classification, quantification and prognosis. Our work considers SHM quantification level and in particular the evaluation of the severity of delamination-type damage in CFRP composite laminates. Prior to quantification algorithms implementation, it is important to properly prepare the supports on which algorithms will be tested. Teflon inserts and conventional impacts are commonly used techniques to generate or simulate delaminations. However, with such rudimentary techniques it is difficult to generate controlled delamination-type damage in a realistic way. In the present work, we investigate symmetrical laser shock approach, as a new method to calibrate delaminations in composites. By tuning the time delay between the two laser beams and laser energy, through-thickness damage position and severity can respectively be adjusted. The effect of multiple contiguous laser impacts was also investigated. Post-mortem analyses using A-scan and C-scan testing as well as penetrant testing were performed in order to characterize laser impact induced damage. Results are encouraging and demonstrate the high potential of symmetrical laser shock for damage calibration in both size and location.

1. Introduction

Due to their low density, high specific strength and stiffness, long fatigue and high creep, corrosion and temperature resistance, composite materials are increasingly used in various industrial fields and especially in aeronautics. For commercial aircrafts, the percentage of fiber-reinforced composite materials used in the latest Boeing B787 and newly designed Airbus A350-XWB reaches 50% and 52% respectively [1]. Despite having great advantages, composite materials are not exempt from drawbacks. Particularly, composites can be subject to various types of damage such as fiber breakage, matrix cracking, fiber–matrix debonding, and delamination between plies [2]. Most of these damages, particularly delamination-type damage, occur beneath the top surface and are barely or even not visible. They can, however, severely degrade the performance of composites and should be identified in time in order to avoid catastrophic structural failures. Therefore, the application of automatic damage monitoring strategies to composites is crucial. The process of implementing such automatic damage detection and characterization strategies is referred to as Structural Health Monitoring (SHM) [3]. SHM can be defined as the process of acquiring and processing data from on-board sensors to evaluate the health of a structure. The major characteristic inherent to any SHM system is that sensors have to be embedded or permanently attached to the monitored structure, leading to the main advantages of SHM compared to traditional Non-Destructive Testing (NDT): automated inspection process, increased asset readiness and large savings in maintenance costs. SHM process can be regarded as a hierarchy of levels which are as follows [4,5]:

- Level 1 Detection: Recognition that damage might be present in the structure
- Level 2 Localization: Identification of the probable position of the damage
- Level 3 Classification: Identification of the type of the damage

* Corresponding author.
E-mail address: meriem.ghrib@ensam.eu (M. Ghrib).

- Level 4 Quantification: Estimation of the extent of the damage
- Level 5 Prognosis: Estimation of the residual life of the structure

Much of our previous work focused on SHM detection, localization and classification levels [6–8]. Our focus is currently placed on the quantification level and in particular on the assessment of the severity/extent of delamination-type damage in CFRP composite laminates. However, in order to test and validate any quantification approach, physical supports are firstly needed. This paper is thus concerned with the issue of how to generate delamination-type damage that can be calibrated both in size and position. A preliminary study was published in [9]. In the present article, more details are added especially with regards to post-mortem analyses.

In order to test and validate any quantification approach, several solutions have already been proposed by the SHM community. Among them, Teflon inserts and conventional impacts are the major existing techniques used for delamination generation or simulation. In [10], Quaegebeur et al. proposed a structural health monitoring strategy for detecting interlaminar delamination in carbon fiber reinforced polymer structure using Lamb waves. The delamination is simulated by inserting a Teflon tape between two transverse plies and the Lamb wave generation and measurement is enabled by using piezoceramic elements. In [11], a Structural Health Monitoring strategy was proposed in order to detect disbonds in a composite lap-joint. The structure under study is composed of Carbon Fiber Reinforced Polymer (CFRP) bonded to a titanium plate and artificial disbonds are simulated by inserting Teflon tapes of various dimensions within the joint. In-situ inspection is ensured by piezoceramics (PZTs) bonded to the structure. Sohn et al. [12] developed a signal processing technique to detect delamination on composite structures. In particular, a wavelet-based signal processing technique is developed and combined with an active sensing system to produce a near-real-time, online monitoring system for composite structures. For experimental demonstration, delamination on the composite plate was simulated by attaching industrial putties in various locations. It was assumed that the industrial putty patch attenuates the Lamb waves in a similar manner as delamination does and that this material closely models the change of the Lamb wave characteristics that may be expected from delamination. In the study presented in [13], a new delamination detection technique is proposed so that delamination can be detected without using any direct comparison with previously obtained baseline data even in presence of temperature variation. To validate the proposed delamination detection technique, a multi-layer carbon fiber composite plate is considered. A conventional drop-weight impact tester with a steel ball tip is used to introduce low velocity impact damage.

The main weakness with the above stated damage generation techniques is that they do not allow for an effective control of the induced damage. Particularly, the calibration of delamination using conventional impacts is quite difficult. In addition to interlaminar delaminations, conventional impacts may induce other types of damage such as fiber breakage. As for Teflon insert technique, the latter still remain very far from representing a realistic delamination. The induced damage is only a simulation of the real one and excitation-simulated damage interaction may be very different from the one between that same excitation signal and a real damage. As an alternative to conventional damage generation techniques, we thus propose to investigate Laser Shock Wave Technique (LSWT), a new and promising method that can be used to generate calibrated delaminations in composites. The symmetrical laser shock approach was applied to CFRP laminates and a particular emphasis was placed on the effect of time delay and laser beam energies on damage position and severity respectively. The configuration of multiple laser impacts for damage accumulation was also addressed.

The remaining of the paper is organized as follows: Firstly, principle and fundamentals of LSWT are introduced. Then, the experimental investigations conducted in this study are described. Results and analyses are afterwards presented. Discussion is subsequently provided. Conclusions are finally drawn.

2. LSWT: principle and fundamentals

LSWT consists in a high power laser irradiation of a target. Lasers used for LSWT are high power nanoseconds prototype sources with beam intensities up to several GW/cm^2. The use of such high power lasers generates plasma which induces high pressure shock waves (GPa) inside the target. Such high-pressure shock waves allowed a wide range of applications such as LSP (Laser Shock Peening) [14] and LASAT (LAser Shock Adhesion Test) [15]. LASAT consists of testing material interfaces with laser-driven shock waves. It was first applied to the testing of coating-substrate adhesion [16–18]. More recently, the technique has been applied to composites and the adhesion testing of bonded composites [19]. Gay et al. [20] and Ecault et al. [21] demonstrated that if laser parameters are correctly tuned, a weak bond can be discriminated from a correct one. The work of Bossi et al. [22] also addressed laser bond inspection of bonded composites. However, only the single laser pulse configuration has so far been proposed. The work presented in this paper is based upon the same key principles of LASAT which are:

- Laser-matter interaction and shock wave generation
- Shock wave propagation and controlled damage generation

2.1. Laser-matter interaction and shock wave generation

When a laser pulse, of short duration (ns) and high power (GW) reaches a target, the first few micrometers of the impacted area are transformed into plasma which expands rapidly against the target surface (see Fig. 1). Plasma expansion release creates by reaction a shock wave into the target. The pressure generated by such shock can cover a range from MPa to GPa. In order to drive significant shock pressure, water confinement is generally used. The confinement slows down the plasma expansion and results in an increased ablation pressure (from 5 to 10 times higher compared to the direct irradiation) and a longer shock duration (from 2 to approximately 3 times longer) [23,24]. Furthermore, a sacrificial layer can be interposed between the target surface and the confining medium in order to absorb the plasma induced thermal effects. Usually, an aluminum adhesive is used as a sacrificial layer since laser-aluminum interaction is well documented in literature.

2.2. Shock wave propagation and damage generation

Two configurations of laser shock are distinguishable, according to whether only one side of the target is irradiated (front pulse shock configuration) or both sides of the target are irradiated (symmetrical laser shock configuration).

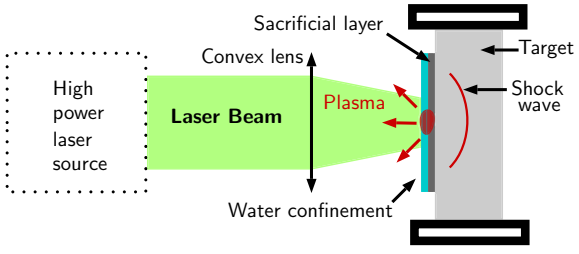

Fig. 1. Laser - matter interaction and shock wave generation.

2.2.1. Front pulse laser shock

Fig. 2 presents a schematic of space–time diagram illustrating the state of stress inside the target at any time and any position. The loading produced by laser impact is a front shock followed by a constant pressure and then a release up to ambient pressure. For simplicity, reflexion/transmission phenomena that occur at ply interfaces are not considered. It should be noted that such assumption is only used to simplify the plot of the time-position diagram and that this is absolutely not a working hypothesis [25,26].

In the case of front pulse laser shock (see Fig. 2), the incident shock wave (S1) created by plasma expansion propagates through the target thickness (e) according to properties depending on the multilayer material characteristics and geometry [27]. When reaching the sample back face which is a zero acoustic impedance frontier, (S1) is reflected into a release wave (R2) propagating backward. Meanwhile, the material front face is unloaded at the end of the pressure pulse. This is also generating a release wave (R1) propagating from the front face to the back face. Depending on the material impedance and thickness, these two release waves (R1 and R2) can intersect inside the material thickness and lead to local high tensile stresses. If the induced tensile stresses are high enough, damage (D) can be created inside the material. It is important to note that the pressure pulse duration is a crucial parameter because it is the one that influences the position of the tensile stress maximum (see Fig. 2) [28]. Thus, in the case of composite targets, if the aim is to localize tensile stresses close to a given interface, pulse duration is the parameter to be tuned. Furthermore, damage severity is directly related to the level of the induced tensile stresses itself linked to the incident laser beam energy. Thus, if the aim is to control damage severity, laser beam energy is the parameter to be monitored.

2.2.2. Symmetrical laser shock

In symmetrical laser shock configuration, both left (L) and right (R) sides of the target are irradiated (see Fig. 3). The incident shock wave (SL) created by plasma expansion which is generated by the left pulse, propagates through the target thickness. When reaching the sample right face, (SL) is reflected into a release wave denoted by (R-SL). Similarly, the incident shock wave (SR) created by the right pulse is reflected into a release wave (R-SR) once it reaches the sample left face. The crossing of the two release waves (R-SL) and (R-SR) creates local high tensile stress which, if high enough, can result in damage (D-SHM) at a through thickness depth (P). Meanwhile, the sample left face is unloaded at the end of the left pressure pulse. This is generating a release wave (RL) propagating from the left face to the right one. This also applies to the right face. The latter is unloaded at the end of the right pulse which is creating a release wave (RR) propagating from the right face to the left face. The crossing of (RR) and (R-SR) can result in damage (DL) close to the left side of the sample in the case the induced tensile stresses by such crossing overpass the material damage threshold. Likewise, the intersection between (RL) and (R-SL) can result in damage (DR) close to the sample right face.

From the time-position diagrams presented in Fig. 3, it can be seen that by tuning time delay between the two laser pulses, the position of the tensile loading zones and hence the position of damage through the thickness of the irradiated material can be adjusted. The left diagram illustrates the case of the symmetrical laser shock with zero time delay. If we focus only on the position of D-SHM, we can see that the latter occurs at the average sample depth. The right diagram presents the case where a non-zero delay denoted by (TD) is introduced between pulses. In this case, the position of D-SHM is shifted by a distance denoted by (DO). Theoretically, in a 1D approach that neglects the transmission/reflection phenomena, the product of half-time delay ($\frac{1}{2}TD$) and speed of sound in the material (C) gives the offset in depth (DO) relative to the average sample depth.

$$DO = \frac{1}{2}TD \times C \tag{1}$$

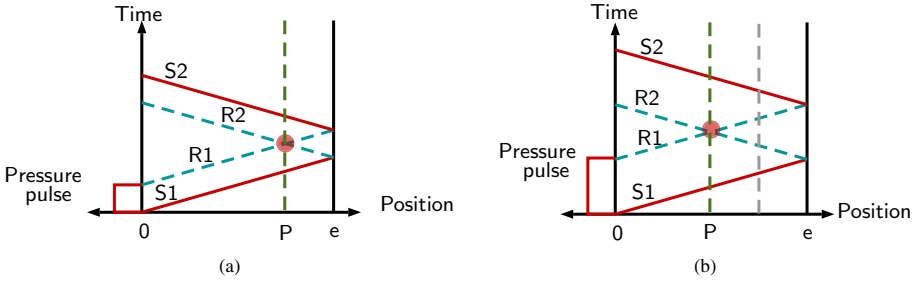

Fig. 2. Time/position diagrams in the case of one pulse laser shock – pressure pulse duration is longer in (b) than in (a).

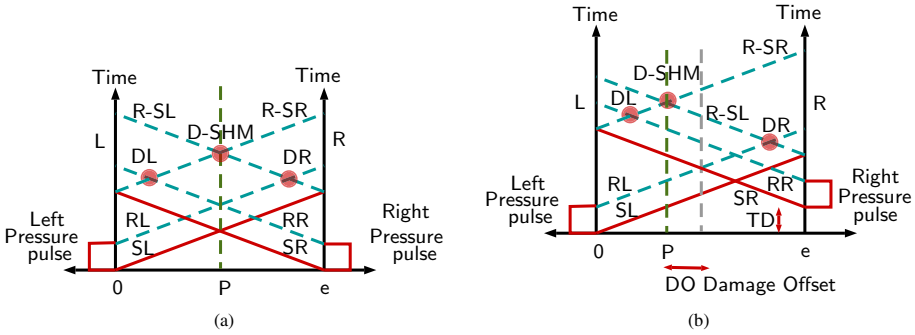

Fig. 3. Time/position diagrams in the case of symmetrical laser shock- (a): zero time delay, (b): Non zero time delay.

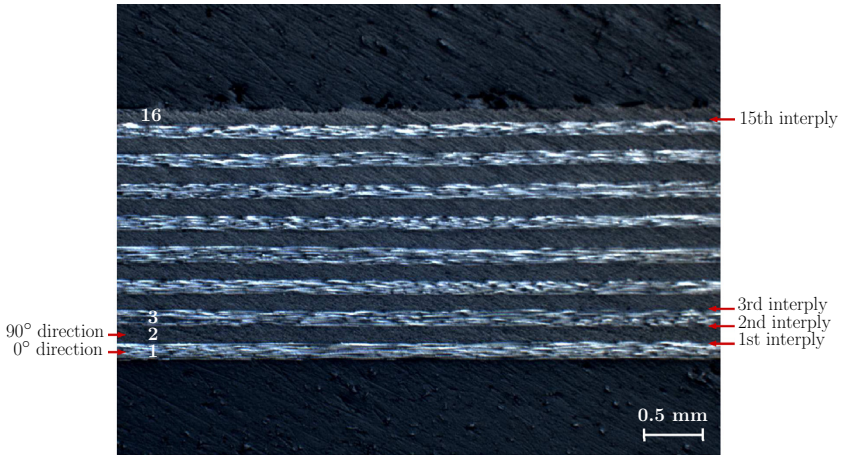

Fig. 4. Cross-sectional microscopy of a test sample.

Thus if the aim is to localize tensile stresses close to a given interface, time delay is the parameter to be monitored while laser beam energies are the parameters to be tuned in order to control the induced damage severity. For SHM assessment purposes, it would be convenient to induce only D-SHM and control its depth and extent.

3. Experimental investigation

3.1. Test samples

The samples considered in this work are CFRP laminates used in aeronautical industry. They are made of 16 unidirectional plies stacked in $(0°, 90°)$ sequence (Fig. 4). Samples have dimensions of 50 mm × 50 mm × 2.2 mm. Test samples material properties are illustrated in Table 1:

3.2. Material characterization

3.2.1. A-scan ultrasonic testing

In order to characterize the presence of laser impact induced damage, multiple A-scan ultrasonic testing were conducted using a single element transducer emitting at 10 MHz in pulse echo mode. A variable called "damage echo visibility" takes the value of zero when no damage echo is observed between the initial pulse and the back echo pulse, a value of one when a damage echo is clearly observed and a value between zeo and one when the damage echo is not clearly distinguished.

3.2.2. C-scan ultrasonic testing

To characterize laser impact induced damage, namely its size and depth, C-scan ultrasonic cartographies were performed using a 10-MHz, 64-elements phased-array transducer in the pulse echo mode (Fig. 5). NDTKit software developed at Airbus group and distributed by Testia as Ultis [29], processed C-scan raw data (Fig. 5) and allowed access to damage surface (mm^2), outline surface (mm) which corresponds to the area of the smallest rectangle surrounding the damage, outline length (mm), damage median depth (mm) and standard deviation of damage depth.

Table 1
Test samples material properties.

Poisson's ratio ν	0.3
Fibre density	1.79
Resin density	1.3
Fibre volume fraction	60%
E_{11}(per ply)	140 GPa
E_{22}(per ply)	9 GPa
E_{12}(per ply)	4.5 GPa

3.2.3. Penetrant testing

For post-mortem analyses, cross-sectional observations and penetrant testing were also considered. Each irradiated sample is cut at the middle of the impact trace distinguished by a slight change in the surface color (Fig. 6). Penetrant testing was performed since it allows for a higher contrast. In our case, the penetrant which has been used is the Babbco WB-200: a fluorescent self-revealing penetrant. Observations were conducted under UV lighting.

3.3. Laser source

Laser shock experiments were conducted at PIMM Hephaistos facility. The laser source (Gaia HP from Thales Company) delivers two beams of 7 joules at 532 nm. The laser pulse has a Gaussian temporal profile with 10 ns duration at half maximum. Time delay between the two laser beams can be tuned from 0 to few µs.

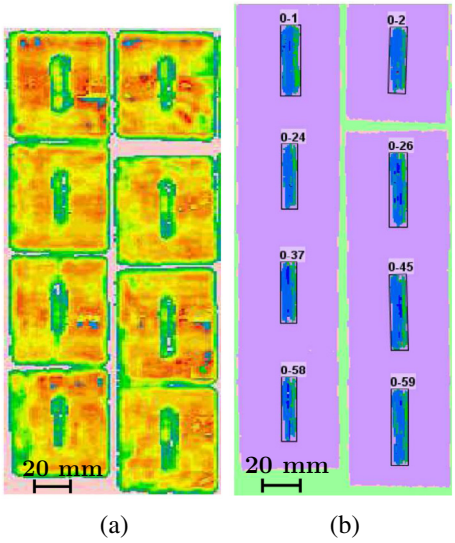

Fig. 5. Example of C-scan cartographies: (a) before processing, (b) after processing.

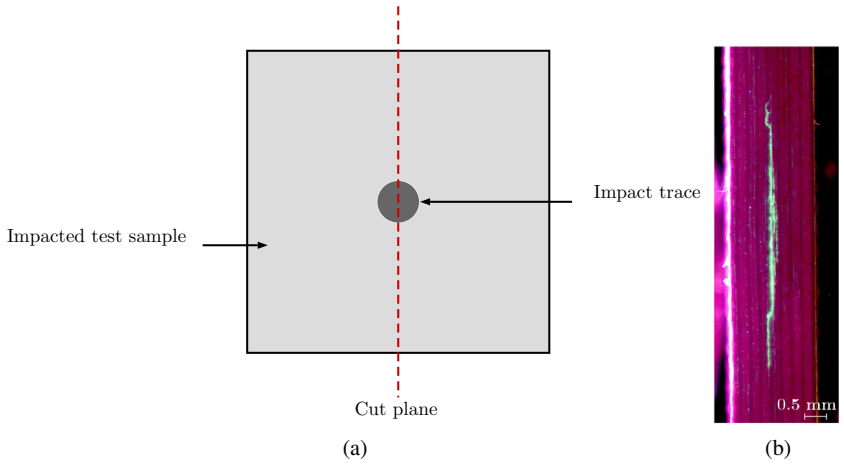

Fig. 6. (a) Position of the cut plane (b) Example of PT/Cross-sectional observation.

3.4. Experimental laser shock configurations

Let A and B be the laser channels as shown in Fig. 7. The two laser beams are focused on the target by means of two convergent lenses, each of 150 mm focal length. A distance of 12.8 cm separates the test sample from each lens which corresponds to 6 mm diameter irradiation spots. Laser irradiations were performed in water confinement configuration and an aluminum painting was used as a sacrificial layer.

Four series of laser impacts were considered.

Series 1: Research of damage threshold In this paragraph, the damage threshold of our test samples is investigated. Two damage thresholds are defined according to whether the laminate is subject to:

- One laser pulse (Only one laser channel (A or B) is activated)
- Symmetrical laser pulses (Both laser channels (A and B) are activated)

This step is crucial since it will allow as to adequately tune our laser parameters in order to avoid near to surface damages (DL and DR on Fig. 3) while still having D-SHM. The samples were subject to increasing laser intensities. For each laser intensity, the irradiated sample was recovered from the experimental room and analyzed using an A-scan ultrasonic testing.

Series 2: Time delay effect In order to study the effect of time delay, a series of symmetrical impacts was considered at constant beam energies, namely 50% of the maximum intensity of each laser channel, and various time delays. As mentioned in Eq. 1, the product $\frac{1}{2}TD \times C$where $C$is the speed of sound in the material, gives the damage offset in depth relative to the average sample thickness. Hence, in the case of our material for which $C$is estimated to be equal to 3×10^{-3} mm/ns [26], a time delay of 80 ns, for instance, will shift the damage position by $\frac{1}{2} \times 80 \times 3 \times 10^{-3} = 0.12$ mm which corresponds to

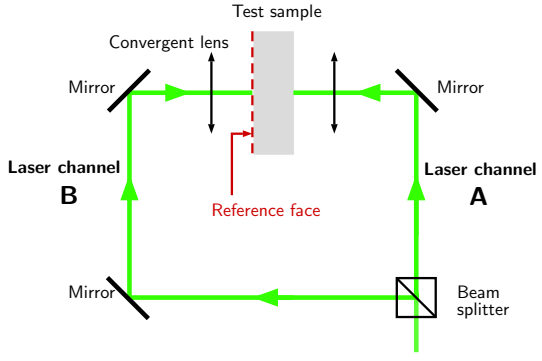

Fig. 7. Experimental set-up.

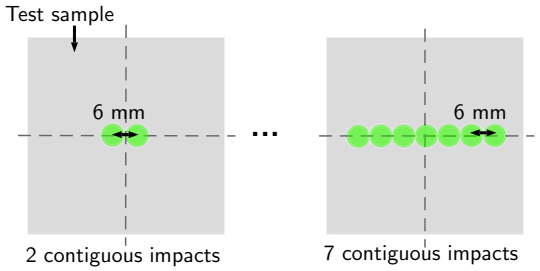

Fig. 8. Schematic of multiple laser impacts configuration.

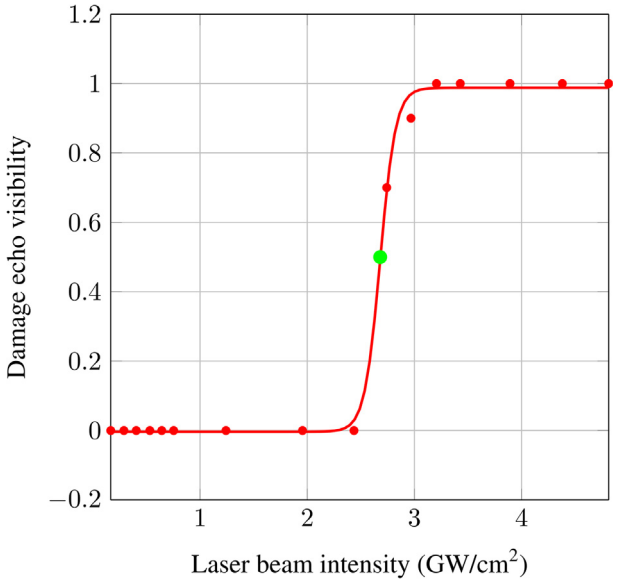

Fig. 9. Damage echo visibility as function of laser beam intensity: Damage threshold in the case of one laser pulse.

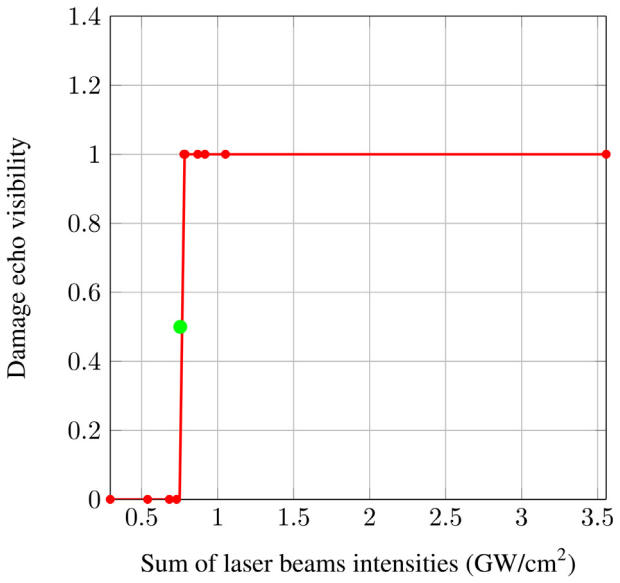

Fig. 10. Damage echo visibility as function of sum of laser beams intensities: Damage threshold in the case of symmetric pulses.

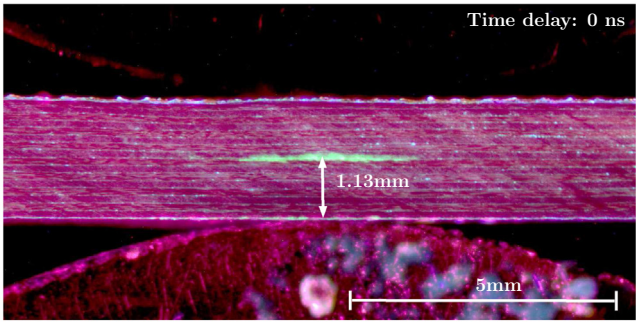

Fig. 11. Damage depth in the case of symmetrical laser shock configuration and zero time delay.

approximately one ply thickness. More generally, a time delay of $n \times 80$ ns will shift the damage position by $n \times \frac{1}{2} \times 80 \times 3 \times 10^{-3} = \mathrm{n} \times 0.12$ mm, which corresponds to the thickness of n plies. In this paper, time delays of 0 ns, 80 ns, 160 ns and 240 ns were considered. For repeatability analysis, each time delay configuration was tested five times. Post-mortem analyses using C-scan ultrasonic testing as well as penetrant testing were conducted in order to estimate through thickness damage position.

Series 3: Energy effect In order to study the effect of laser beam energies, a series of symmetrical impacts was considered at constant time delay, namely 0 ns, and various beam energies. The energy configurations that have been tested are: 20%, 40%, 60%, 80% and 100% of the maximum intensity of each laser channel. For repeatability analysis, each energy configuration was tested five times. Post-mortem analyses using C-scan ultrasonic testing as well as penetrant testing were also conducted in order to estimate damage size.

Series 4: Multiple laser impacts In this paragraph, we investigate symmetrical laser shock configuration with multiple impacts. In order to accumulate the damage created by each single impact, a series of contiguous impacts as shown schematically on Fig. 8 were conducted. Each single impact was considered at 100% of the maximum intensity of each laser channel and zero time delay between the two laser beams. Series of impacts ranging from 2 to 7 contiguous impacts were considered.

4. Results & analyses

4.1. Research of damage thresholds

Fig. 9 plots the data points obtained while searching for damage threshold under one laser pulse. The horizontal axis corresponds to the intensity of one laser beam (either A or B). The vertical axis corresponds to the variable "damage echo visibility" stated in the section entitled "material characterization". The curve obtained after sigmoid fitting consists of three parts. A first part which corresponds to a laser intensity between 0.2 GW/cm^2 and 2.4 GW/cm^2. For such intensity range, no damage echo was

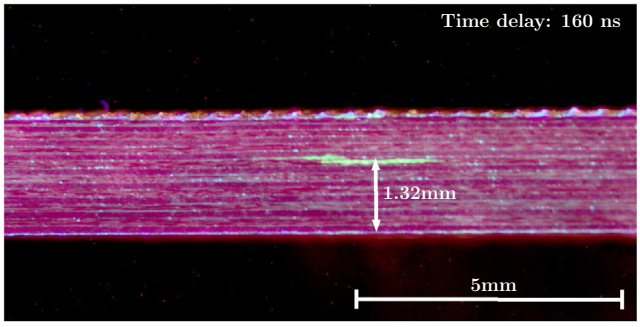

Fig. 13. Damage depth in the case of symmetrical laser shock configuration and 160 ns time delay.

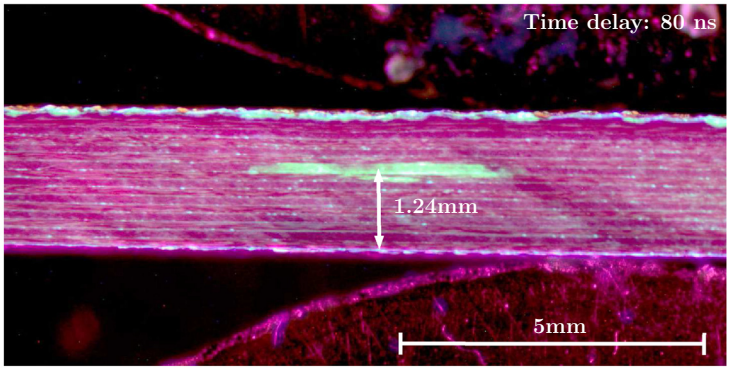

Fig. 12. Damage depth in the case of symmetrical laser shock configuration and 80 ns time delay.

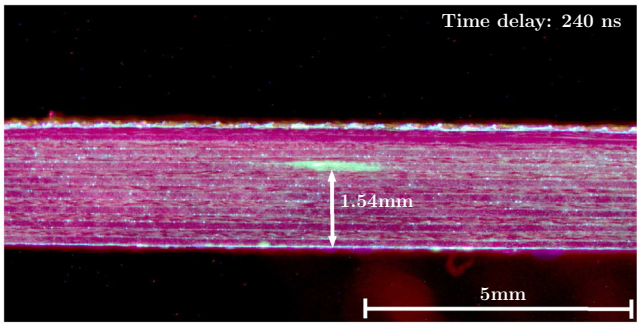

Fig. 14. Damage depth in the case of symmetrical laser shock configuration and 240 ns time delay.

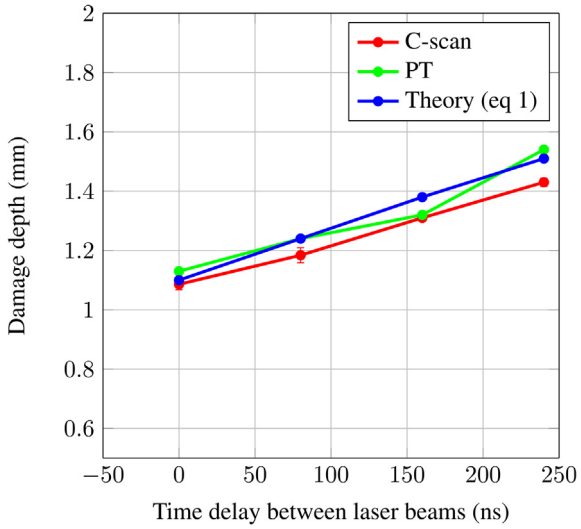

Fig. 15. Damage depth as function of time delay between the two laser beams: Time delay effect at constant laser energy (50% of the maximum intensity of each laser channel).

observed under A-scan testing. The second part corresponds to a laser intensity in the range of 2.4 GW/cm^2 to 3.2 GW/cm^2. Within this interval, a damage echo was observed but not in a very clear way. Finally, the third part corresponds to a laser intensity higher than 3.2 GW/cm^2. For such intensity values, a damage echo was clearly observed. If one assumes that the damage threshold of our test samples when they are subject to one laser pulse ($Thresh_{one-pulse}$)coincides with the 50% point after sigmoid fitting, then $Thresh_{one-pulse}$corresponds to a laser intensity of 2.7 GW/cm^2.

Fig. 10 illustrates a similar result as in Fig. 9 except that the horizontal axis of Fig. 10 corresponds to the sum of laser intensity of channel A and laser intensity of channel B since in this case the sample is under the solicitation of both laser channels simultaneously. The variable "damage echo visibility" is plotted against the sum of laser beams intensities and similarly, a sigmoid curve is fitted to data points. If one assumes that the damage threshold of our test samples when they are subject to symmetrical laser pulses ($Thresh_{sym-pulses}$)coincides with the 50% point, then $Thresh_{sym-pulses}$corresponds to a laser intensity of 0.76 GW/cm^2.

We note that the damage threshold under symmetrical laser impacts is significantly lower than in the case of single laser impact. Thus, in the symmetrical laser shock configuration and if the laser intensity falls in the range $[Thresh_{one-pulse}, Thresh_{sym-pulses}]$, it is expected that near to surface damages, that is DL and DR (Fig. 3), will not occur while still having D-SHM.

4.2. Time delay effect

For the various time delay configurations that were tested, the irradiated samples were analyzed using C-scan ultrasonic testing as well as PT/cross sectional observations.

Figs. 11–14 show that a zero time delay corresponds to a delamination that occurs at the average sample depth while a non-zero time delay induces a damage offset. For example, a delay of 80 ns corresponds to a damage depth of 1.24 mm and a 240 ns time delay corresponds to a damage depth of 1.54 mm. Fig. 15 illustrates the theoretical (Eq. 1) as well as the experimental curves of damage depth as a function of time delay. The experimental results thus obtained show that, as expected, the tuning of time delay allows the adjusting of through thickness damage position. Furthermore, there is a good match between theoretical and experimental results. Thus, Eq. 1 can be used to make prior choices of time delay.

4.3. Energy effect

For the various energy configurations that were tested, the irradiated samples were analyzed using C-scan ultrasonic testing as well as PT/cross sectional observations. Figs. 16–20 illustrate cross sectional observations for various energy configurations. For 20% of the maximum intensity of each laser beam, the induced damage is 3.57 mm long. The damage length increases as long as we keep increasing the intensity of each laser beam until it reaches a value of 6.54 mm for 100% of the maximum laser intensity. It is interesting to note a slight crookedness in damage shape in Fig. 20. This could be explained by edge effects which translate into a significant shear loading resulting in intralaminar cracks occurring at the edges of the main delamination. This point needs to be further investigated in future work.

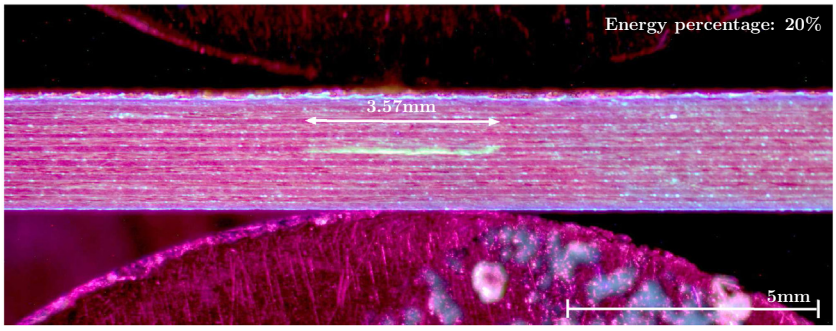

Fig. 16. Damage size in the case of symmetrical laser shock configuration and 20% energy percentage.

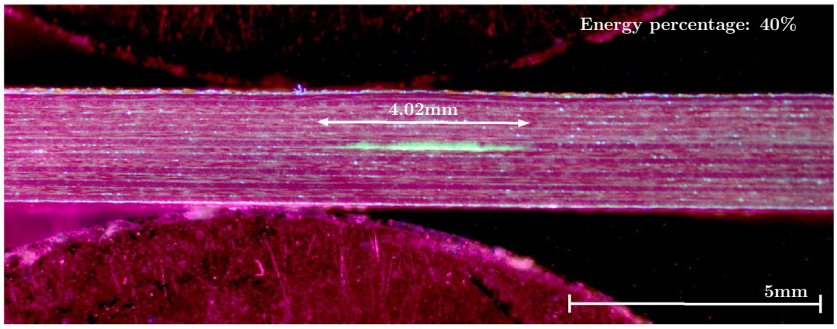

Fig. 17. Damage size in the case of symmetrical laser shock configuration and 40% energy percentage

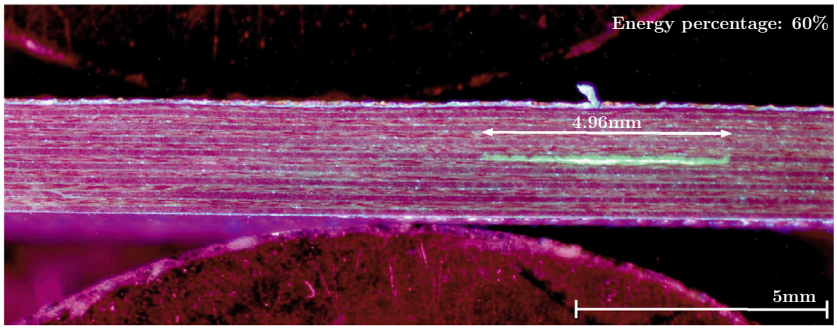

Fig. 18. Damage size in the case of symmetrical laser shock configuration and 60% energy percentage.

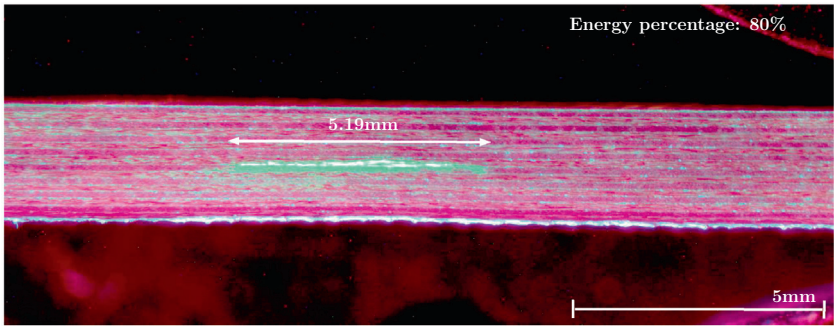

Fig. 19. Damage size in the case of symmetrical laser shock configuration and 80% energy percentage.

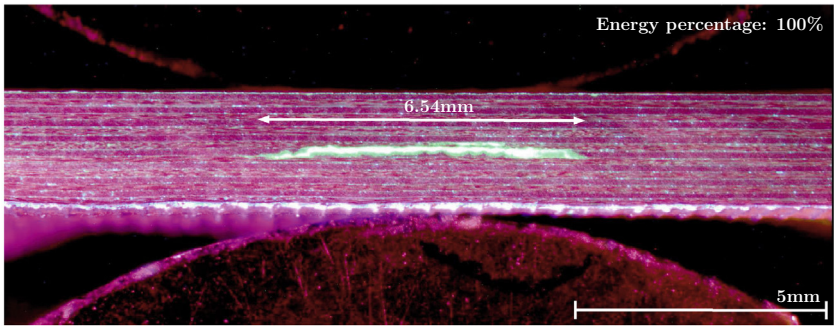

Fig. 20. Damage size in the case of symmetrical laser shock configuration and 100% energy percentage.

Fig. 21 plots damage outline length estimated by C-scan as well as damage length estimated by penetrant testing, against the sum of the two laser beams intensities. Damage size estimated by C-scan is around 9 mm if 20% of the maximum intensity is considered at each laser channel. Then, damage size increases linearly with laser intensity until it reaches a length of approximately 16 mm for 100% of the maximum laser intensity. Based on PT analyses damage size is between 3.5 mm and 6.5 mm. Damage size

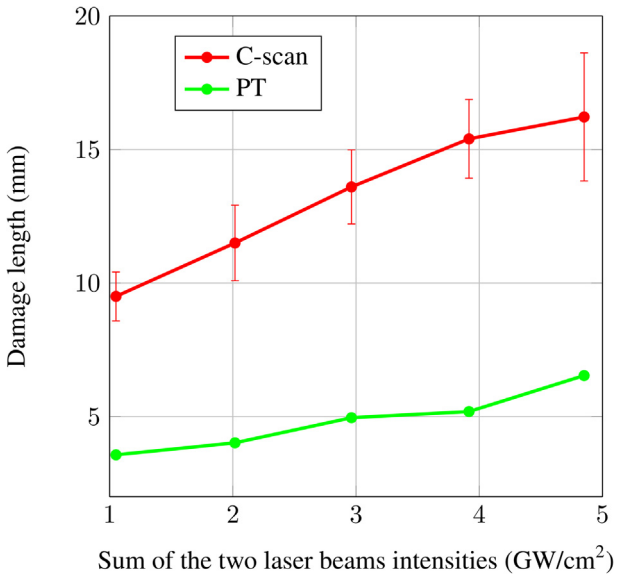

Fig. 21. Damage length against sum of the two laser beams intensities.

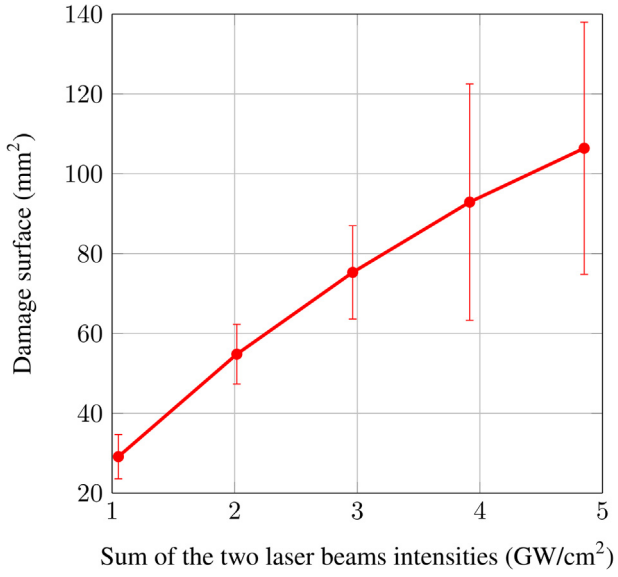

Fig. 22. C-scan estimated damage surface against sum of the two laser beams intensities.

estimated by C-scan is higher than that estimated by PT analyses. This could be explained by the fact that with PT tests, it is difficult to visualize the micro-delaminations that appear at the edges of the main delamination. This is inherent to the nature of PT analyses which provide better contrast but not a good resolution. C-scan analyses, however, can capture these micro-delaminations.

Fig. 22 plots C-scan estimated damage surface (mm^2) as a function of the sum of the two laser beams intensities. It can be seen that for 20% of the maximum laser intensity at each channel, damage surface is around 30 mm^2. Then, damage surface increases in a linear way with laser energy until it reaches a value of approximately 105 mm^2. We also draw attention to the maximum damage size obtained. If we consider damage length (Fig. 21), the latter is estimated by C-scan testing to be around 16.5 mm. In order to get damage sizes of higher values for our future SHM applications, the idea was to accumulate damage by multiple contiguous laser impacts.

4.4. Multiple laser impacts

Figs. 23–29 illustrate cross sectional observations for an increasing number of contiguous laser impacts. For one symmetrical laser impacts, PT-estimated damage length is around 7.3 mm. By increasing the number of contiguous laser impacts, damage length tends to grow. For seven contiguous laser impacts, the accumulated damage is 41.7 mm long. This trend is also illustrated in Fig. 30 which plots laser contiguous impacts number versus C-scan and PT estimated damage size. A gap is similarly noticed between C-scan and PT estimated damage lengths. With PT analyses we tend to underestimate the size of the damage. The same argument given in the section above can apply herein. The obtained results demonstrate that the approach of multiple laser impacts appears promising when applied to damage accumulation and consequently to damage size control.

5. Discussion

This work discussed Laser Shock Wave Technique as a novel way to generate controlled delamination in CFRP composites. Particular attention was paid to symmetrical laser shock configuration. We addressed not only the effect of time delay between laser beams on damage depth but also the effect of laser energy on damage size. LSWT has been applied to various fields such as LASAT. To our knowledge, this is the first study to deal with its application to damage calibration. The findings of our research are quite convincing, and thus the following conclusions can be drawn:

- The symmetrical laser shock is a good alternative to conventional damage generation techniques thus opening new perspectives for SHM applications.
- An adequate tuning of laser parameters, namely laser energy (intensity) and time delay, allows for a good monitoring of damage size and through thickness damage position respectively.

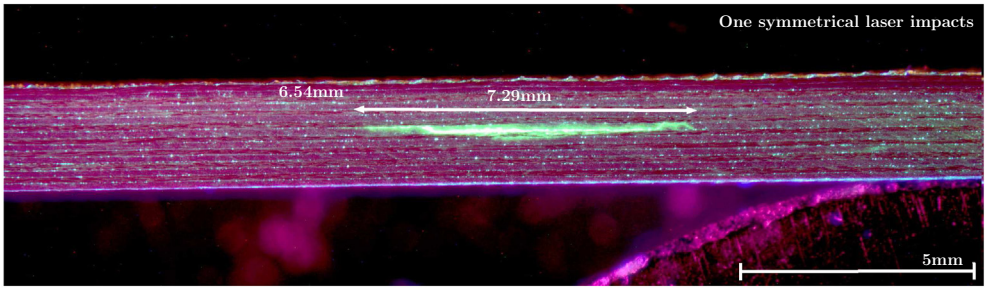

Fig. 23. Damage size in the case of one symmetrical laser shock.

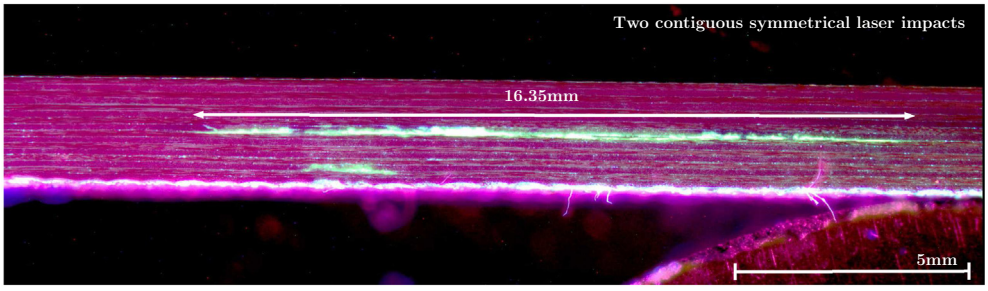

Fig. 24. Damage size in the case of two contiguous symmetrical laser impacts.

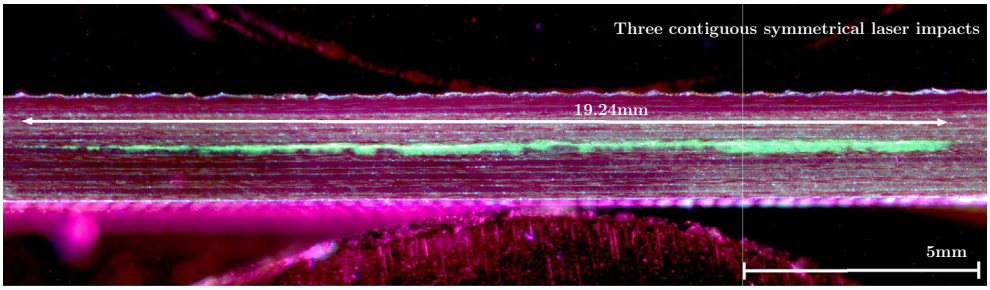

Fig. 25. Damage size in the case of three contiguous symmetrical laser impacts.

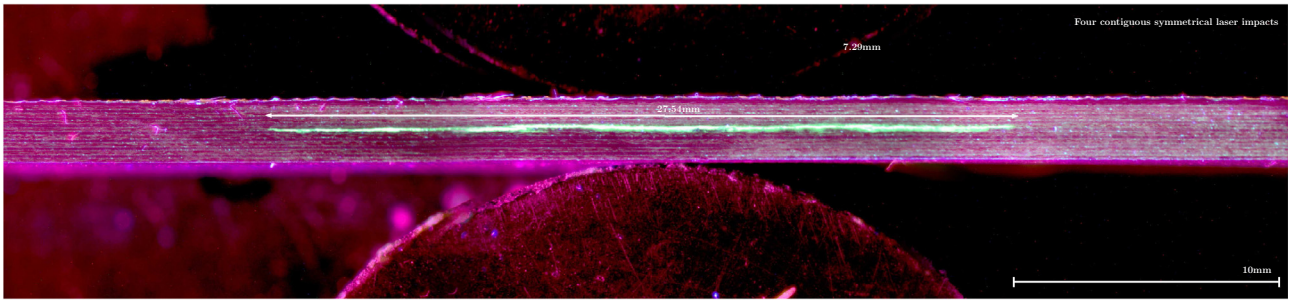

Fig. 26. Damage size in the case of four contiguous symmetrical laser impacts.

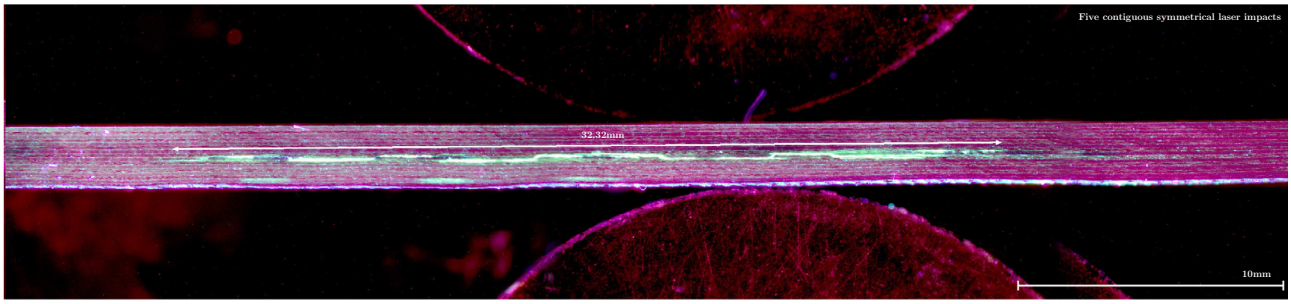

Fig. 27. Damage size in the case of five contiguous symmetrical laser impacts.

- Multiple laser impacts are a good trick to combine single impact induced damage.

LSWT could potentially be applied to sandwich composites in order to introduce realistic and controlled disbonds between skin and core material. A careful choice of laser parameters is a key factor in the application of high power laser sources for damage generation and calibration. Such choice should be based on prior numerical simulation results also called "predictive simulations". Hence numerical models adjusted based on experimental measurements are needed. In this regard, one can cite ESTHER code developed by CEA. ESTHER is one of the very few codes, if not the only one, that deals with 1D simulation of materials under very high power laser irradiation [30]. One can also cite LS-DYNA code for 2D or 3D simulations of composites under high power laser shock [26]. Laser parameters optimization is a key step toward the development of a reliable and controlled laser shock wave technique for damage calibration. But up until now, very little

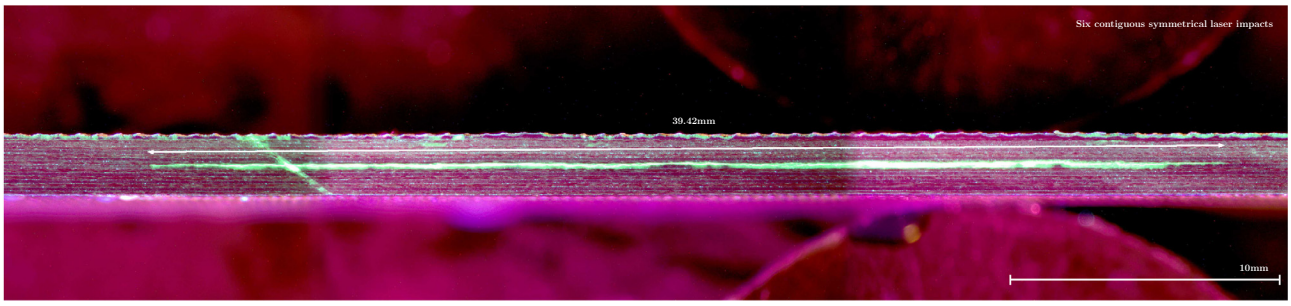

Fig. 28. Damage size in the case of six contiguous symmetrical laser impacts.

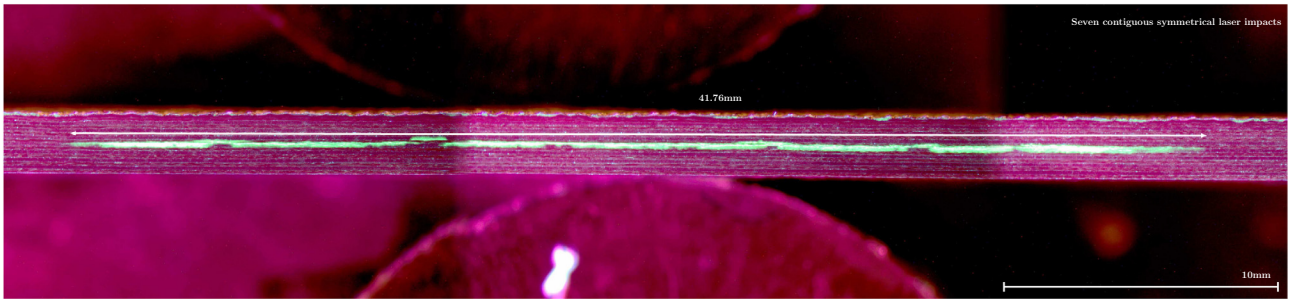

Fig. 29. Damage size in the case of seven contiguous symmetrical laser impacts.

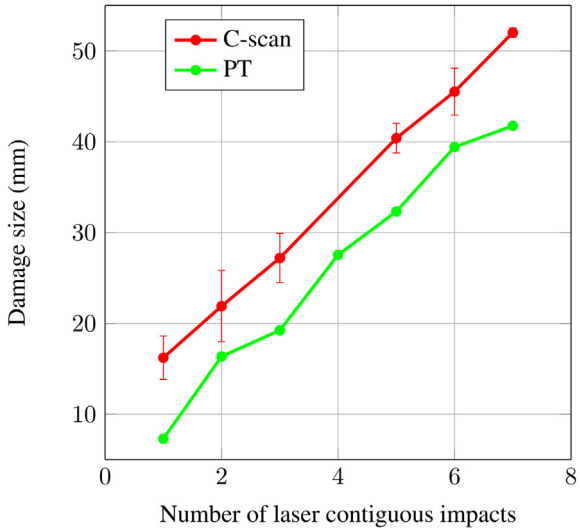

Fig. 30. Damage length versus number of contiguous laser impacts.

work has been conducted on this topic and further research must take place in order to address the issue of laser parameters control and optimization.

6. Conclusions

In this study, it was experimentally demonstrated that LSWT is an effective technique for delamination generation and calibration in composites. A-scan and C-scan ultrasonic testing as well as penetrant testing were selected for post-mortem analyses. Future analyses may include tomography and acoustic microscopy to get deeper insights about damage internal features. Finally, predictive simulations recalibrated based on the experimental results presented in this work may be conducted to address laser parameters control and optimization.

Acknowledgements

The authors would like to thank Yann Rouchausse, a member of the laser shock team at PIMM laboratory for his support during experimental investigations and also to express their gratitude to Patrick Israel, a member of R&T composites laboratory of Material and Processes department of SAFRAN Nacelles company for his help during PT/cross sectional post-mortem analyses.

References

[1] Cai Jian, Qiu Lei, Yuan Shenfang, Shi Lihua, Liu Peipei, Liang Dong. Structural health monitoring for composite materials. In: Composites and their applications, chapter structura. InTech; 2012. p. 37–60.
[2] Ramesh Talreja, Veer Singh Chandra. Damage and failure of composite materials. Cambridge University Press; 2012.
[3] Farrar Charles R, Worden Keith. An introduction to structural health monitoring. Philos Trans R Soc 2007;365:303–15 (December 2006).
[4] Rytter Anders [Ph.D. thesis]. Aalborg universitet vibrational based inspection of civil engineering structures rytter anders. Aalborg: Aalborg University; 1993.
[5] Worden Keith, Manson Graeme. The application of machine learning to structural health monitoring. Philos Trans R Soc A: Math Phys Eng Sci 2007;365:515–37 (December 2006).
[6] Mechbal Nazih, Uribe Juan Sebastian, Rébillat Marc. A probabilistic multi-class classifier for structural health monitoring. Mech Syst Signal Process 2015;60:106–23.
[7] Bakir Myriam, Rebillat Marc, Mechbal Nazih, Bakir Myriam, Rebillat Marc, Mechbal Nazih. Damage type classification based on structures nonlinear dynamical signature. In: 9th IFAC symposium on fault detection, supervision and safety of technical processes. p. 657. Paris.
[8] Hajrya Rafik, Mechbal Nazih. Perturbation analysis for robust damage detection with application to multifunctional aircraft structures. Smart Struct Syst 2015.
[9] Ghrib Meriem, Berthe Laurent, Marc R, Mechbal Nazih, Guskov Mikhail. Laser shock a novel way to generate calibrated delamination in composites : concept & first results. In: EWSHM, number July. p. 5–8.
[10] Quaegebeur N, Micheau P, Masson P, Maslouhi A. Structural health monitoring strategy for detection of interlaminar delamination in composite plates. Smart Mater Struct 2010;19:085005 (June).
[11] Quaegebeur N, Philippe M, Masson P, Belanger H. Structural health monitoring of bonded composite joints using piezoceramics. In: Smart Materials, Structures & NDT in Aerospace, number November, 10.
[12] Sohn Hoon, Park Gyuhae, Wait Jeannette R, Limback Nathan P, Farrar Charles R. Wavelet-based active sensing for delamination detection in composite structures. Smart Mater Struct 2003;13:153–60.

[13] Yeum Chul Min, Sohn Hoon, Ihn Jeong Beom, Lim Hyung Jin. Instantaneous delamination detection in a composite plate using a dual piezoelectric transducer network. Compos Struct 2012;94:3490–9 (May 2016).
[14] Fabbro R, Peyre P, Berthe L, Scherpereel X. Physics and applications of laser-shock processing. J Laser Appl 1998;10.
[15] Berthe L, Arrigoni M, Boustie M, Cuq-Lelandais JP, Broussillou C, Fabre G, et al. State-of-the-art laser adhesion test (LASAT). In: Nondestructive Testing and Evaluation.
[16] Barradas S, Jeandin M, Bolis C, Berthe L, Arrigoni M, Boustie M, Barbezat G. Study of adhesion of PROTAL copper coating of Al 2017 using the laser shock adhesion test (LASAT). J Mater Sci 2004;39:2707–16.
[17] Barradas Sophie, Molins R, Jeandin M, Arrigoni M, Boustie M, Bolis C, Berthe L, Ducos M. Application of laser shock adhesion testing to the study of the interlamellar strength and coating-substrate adhesion in cold-sprayed copper coating of aluminum. Surf Coat Technol 2005;197:18–27.
[18] Guipont Vincent, Jeandin Michel, Bansard Sebastien, Khor Khiam Aik, Nivard Mariette, Berthe Laurent, Cuq-Lelandais Jean Paul, Boustie Michel. Bond strength determination of hydroxyapatite coatings on Ti-6Al-4V substrates using the LAser Shock Adhesion Test (LASAT). J Biomed Mater Res – Part A December 2010;95(4):1096–104.
[19] Toller Steven M, Dulaney Jeff L. Laser induced bond delamination; 2012.
[20] Gay Elise, Berthe Laurent, Boustie Michel, Arrigoni Michel, Trombini Marion. Study of the response of CFRP composite laminates to a laser-induced shock. Compos Part B: Eng 2014;64:108–15.
[21] Ehrhart Bastien, Ecault Romain, Touchard Fabienne, Boustie Michel, Berthe Laurent, Bockenheimer Clemens, Valeske Bernd. Development of a laser shock adhesion test for the assessment of weak adhesive bonded CFRP structures. Int J Adhes Adhes July 2014;52:57–65.
[22] Bossi R et al. Laser bond testing. Mater Eval 2009.
[23] Berthe L, Fabbro R, Peyre P, Tollier L, Bartnicki E. Shock waves from a water-confined laser-generated plasma. J Appl Phys 1997.
[24] Fabbro R, Fournier J, Ballard P, Devaux D, Virmont J. Physical study of laser-produced plasma in confined geometry. J Appl Phys 1990.
[25] Tarabay Antoun. Spall fracture; 2003.
[26] Ecault Romain, Touchard Fabienne, Boustie Michel, Berthe Laurent, Dominguez Nicolas. Numerical modeling of laser-induced shock experiments for the development of the adhesion test for bonded composite materials. Compos Struct 2016;152:382–94.
[27] Ecault R, Boustie M, Berthe L, Touchard F. Laser shock waves: a way to test and damage composite materials for aeronautic applications. AIP Conf Proc 2012;126:126–37.
[28] Gay Elise, Berthe Laurent, Boustie Michel, Arrigoni Michel, Trombini Marion. Study of the response of CFRP composite laminates to a laser-induced shock. Compos Part B: Eng 2014;64:108–15.
[29] Silvère Barut, Nicolas Dominguez, NDT Diagnosis Automation : a Key to Efficient Production in the Aeronautic Industry; 2016.
[30] Bardy Simon, Aubert Bertrand, Berthe Laurent, Combis Patrick, Hébert David, Lescoute Emilien, Rullier Jean-Luc, Videau Laurent. Numerical study of laser ablation on aluminum for shock-wave applications: development of a suitable model by comparison with recent experiments. Opt Eng 2016;56(1):011–4.